State-of-the-art efficiency determination of a wind turbine drivetrain on a nacelle test bench

Hongkun Zhang[1], Paula Weidinger[2], Christian Mester[3], Zihang Song[2], Marcel Heller[1],
Alexander Dubowik[2], Bernd Tegtmeier[1], and Karin Eustorgi[1]

[1]Fraunhofer Institute for Wind Energy Systems IWES, 27572 Bremerhaven, Germany
[2]Physikalisch-Technische Bundesanstalt, Braunschweig, Germany
[3]Federal Institute of Metrology METAS, 3003 Bern-Wabern, Switzerland

Correspondence: Karin Eustorgi (karin.eustorgi@iwes.fraunhofer.de)

Abstract. The efficiency of wind turbine drivetrains is a topic of great interest for both the wind energy industry and the academic community. With the developing maturity of this technology and the increasing pressures to reduce costs, the importance of drivetrain efficiency has grown. However, insufficient accuracy in torque measurement makes actually determining the efficiency of wind turbine drivetrains a very challenging task. In the project known as WindEFCY, state-of-the-art measurement
5 and calibration instruments are used to determine the drivetrain efficiency of a direct drive wind turbine on the nacelle test bench called the DyNaLab. This paper discusses the test configuration applied for this work as well as the instrumentation of the measurement systems used. It further presents the results from two tests of different types to demonstrate the process of efficiency determination and the analysis of uncertainty. Within the paper's scope of study, an uncertainty level of approximately 0.7% is achievable when measuring drivetrain efficiency. Details and recommendations concerning data processing and
10 uncertainty analysis are also given in the paper.

1 Introduction

To further reduce the levelised cost of energy (LCOE), increasing the rated power of a single wind turbine is still a common and effective approach that is actively pursued by the wind energy industry. When developing larger wind turbines, it is of key interest to maximise the efficiency of wind energy utilisation. This efficiency, however, is not a single and constant parameter.
15 Wind turbines operate in a wide working range that at most times deviates from the rated power and speed. Moreover, wind turbines are constantly subjected to stochastic wind conditions that directly or indirectly influence efficiency. The efficiency property of a wind turbine therefore has to be determined across the entire working range and under different conditions. The determined efficiency property provides an important basis for turbine optimisation.

The overall efficiency of the wind turbine consists of the aerodynamic efficiency of the rotor and the efficiency of the drivetrain. The drivetrain efficiency is affected by a number of factors that have to be considered in the design of the turbine. These
20 factors include the setting and functionality of the cooling system, the structural deformation (especially the air gap change for direct drive turbines) due to external loads and temperature change, and the generator and converter control strategies. In order to validate and optimise the turbine design, the influence of these factors on the drivetrain's efficiency needs to be determined

both qualitatively and quantitatively. To do so, it is necessary to determine the efficiency with a high level of accuracy and with
measurements traceable to national standards according to metrological rules (Weidinger et al., 2021).

The best place to determine the drivetrain efficiency of a wind turbine is on a nacelle test bench, where the design mechanical
load cases and electrical grid conditions can be easily produced and replicated. This said, determining efficiency with sufficient
accuracy is still very challenging even on nacelle test benches. One major reason for this is the large measurement uncertainty
(MU) in the torque measurements due to high torque levels and the lack of traceable calibration (Foyer et al., 2019). A few
approaches have been suggested to avoid the need for torque measurement when determining efficiency on nacelle test benches,
including the calorimeter method (Pagitsch et al., 2016) and the modified back-to-back method (Zhang and Neshati, 2018).
Nevertheless, the best method of efficiency determination that is traceable to national standards is still the "direct" method,
i.e., measuring the input and output power directly using state-of-the-art equipment, in this case a 5 MN·m torque transducer
specially developed by PTB, Germany's national metrological institute (Weidinger et al., 2017).

2 Background

The WindEFCY project provided the opportunity to determine the efficiency of a wind turbine with traceable measurements of
both the mechanical input power and electrical output power. The turbine was tested on the 10 MW DyNaLab nacelle test bench
of Fraunhofer IWES in Bremerhaven, Germany. During the test campaign, the 5 MN·m torque transducer (also known as the
torque transfer standard, TTS) as well as other mechanical and electrical sensors were used to produce traceable measurements
of the input and output powers. The efficiency behaviour of the turbine was determined on numerous working points up to
5 MN·m and under different conditions. In addition to aiding the efficiency determination, the availability of the 5 MN·m
TTS also offered a rare chance to calibrate the test bench's own torque transducer, which is instrumented on the shaft adapter
connecting the test bench and the device under test (DUT), as shown in Figure 1. For the calibration, a number of calibration
profiles were also carried out during the test campaign. Since the 5 MN·m TTS is not designed for high levels of non-torque
loads (also known as parasitic loads in some publications), the calibrated test bench transducer could be used instead in future
tests with high non-torque loads.

3 Test layout for efficiency determination

The layout of the complete test setup is depicted schematically in Figure 1. Two motors of the test bench are connected in
tandem to provide the driving torque. A load application unit (LAU) can be used to generate the designed non-torque loads
with a hexapod driven by hydraulics. A coupling is placed between the LAU and the motors to prevent non-torque loads being
transferred backwards to the motors. The non-torque loads are transferred via a main bearing from the hexapod to the output
shaft that also carries the torque. A combination of loads in six degrees of freedom can be applied to the DUT through the flange
of the output shaft. To connect the test bench with the DUT, a shaft adapter is used to fit the flanges on both sides. This adapter
is also used as a robust way to measure loads directly in front of the DUT. For the WindEFCY test campaign, the 5 MN·m
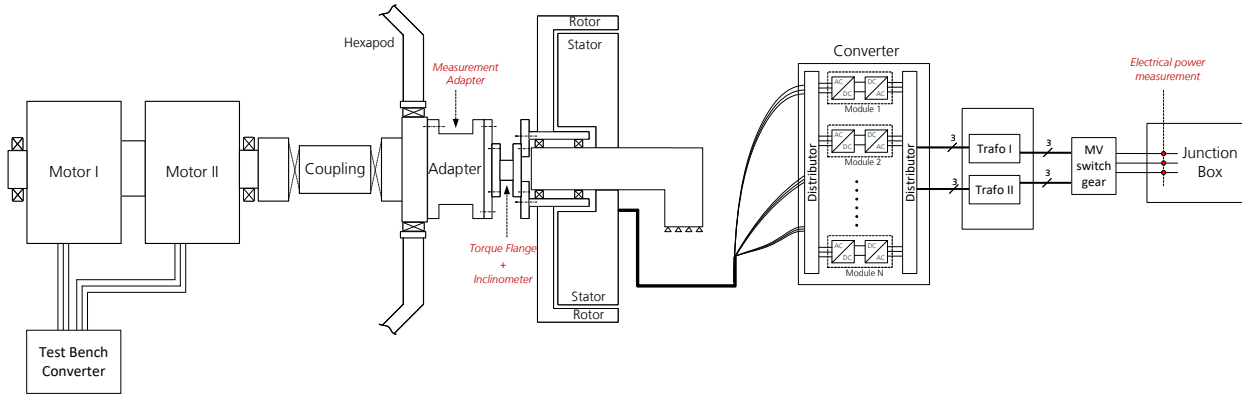
Figure 1. Layout of the test configuration

55   TTS from PTB was additionally integrated into the setup between the shaft adapter and the DUT with the help of specially designed adaptation structures. To protect the 5 MN·m TTS, the applied non-torque load was controlled to the minimum during the tests. The non-rotating part of the DUT is fixed to the base of the test bench. The DUT's generator is electrically connected to a full power converter, which is in turn connected to the transformer. Via a switch gear, the transformer is connected to the medium voltage inside a junction box. For efficiency determination, the mechanical power is measured by the 5 MN·m TTS

60   and the electrical power is measured in the junction box. The efficiency is then determined for all the components in between, including the generator, the converter and the transformer.

4   Measurement of mechanical input power

The mechanical input power of the DUT is a function of the input torque T and the rotational speed ω at the interface of the DUT, as shown in Equation 1. It is very important that the torque and rotating speed being measured at the same position.

65   To this end, a speed measuring channel is also instrumented inside the 5 MN·m TTS with the help of an inclinometer. In this chapter, important details of the torque and speed measurement will be presented.

$$P_{\mathrm{mech}} = T \cdot \omega \tag{1}$$
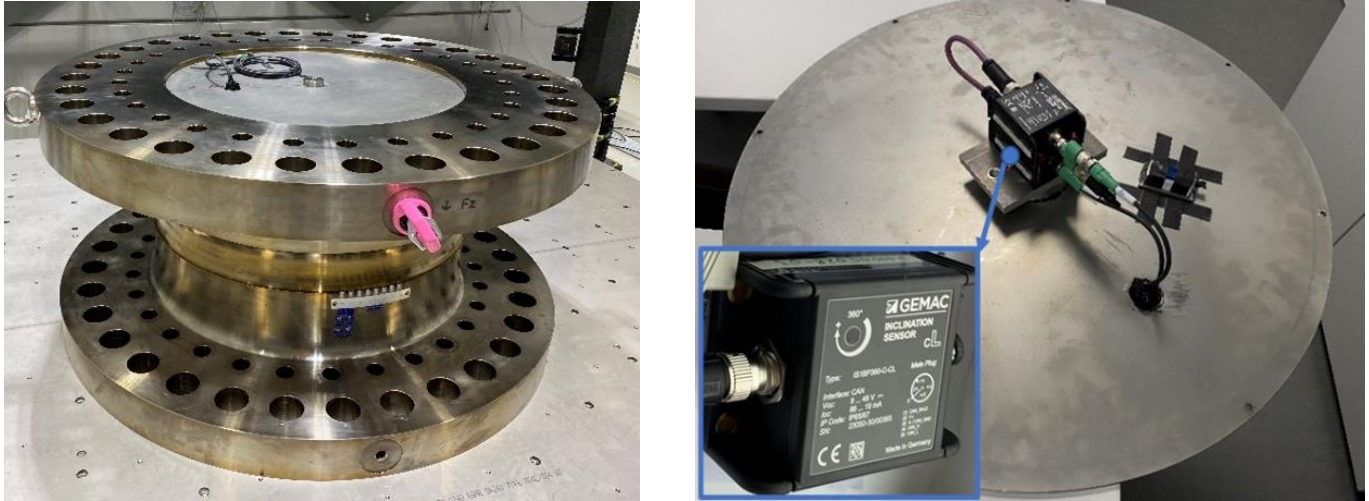
Figure 2. The 5 MN·m flange-type hollow-shaft TTS manufactured by HBM, taken from (Song et al., 2022)

4.1 Torque measurement with the 5 MN·m TTS

To meet the needs of the wind energy industry, a 5 MN·m TTS manufactured by the HBM company was acquired by PTB
especially for use on nacelle test benches. It is pictured in Figure 2 (left). The TTS is equipped with strain gauges applied in
a Wheatstone bridge circuit format to measure torque up to 5 MN·m. Additionally, it can measure bending moment, shearing,
and axial force, but only to a lower level, and these measurements are not traceable to national standards. The TTS is statically
calibrated using PTB's 1.1 MN·m torque standard machine in order to establish a relationship between the transducer's output
signal S_{transd} (in mV/V) and the input torque T_{transd} (in kN·m). This was done according to the torque calibration standard
DIN 51309, but only up to 1.1 MN·m due to the lack of suitable torque standard machines. Because of the very good linearity
(-6.3×10^{-4} at 100 kN·m and 0.7×10^{-4} at 1.1 MN·m) and the very small hysteresis ($< 6.2 \times 10^{-4}$) of the TTS up to 1.1
MN·m, a linear regression curve for increasing and decreasing torque load combined was assumed:

$$T_{\mathrm{transd}} = 3850 \,\mathrm{kN} \cdot \mathrm{m} \cdot \left(\frac{\mathrm{mV}}{\mathrm{V}}\right)^{-1} \cdot S_{\mathrm{transd}} \tag{2}$$

Above 1.1 MN·m, the behaviour of the TTS, including its MU, is predicted by a weighted extrapolated method. In this
method for calibration result extrapolation, the linear regression curve determined in the partial range is used for converting
the mV/V signal into the corresponding torque value. To validate this procedure, a 20 kN·m torque transducer was measured
in three partial (20%, 50%, and 80%) ranges and in the full range, and the relative sensitivities per calibration range were
compared. These absolute differences are in the range of about 3×10^{-6} and thus smaller than the MU of the calibration
itself, which is 3×10^{-5} for case I-A (cubic, smallest MU). The use in the full range of linear regression curves determined in
the partial range is therefore legitimate. In order to check the 5 MN·m TTS's sensitivity stability, it was calibrated in further
sub-ranges (8%, 12%, 16%, and 22%) and the results were compared. The absolute difference in range sensitivity is about

8×10^{-8} and thus noticeably smaller than the overall uncertainty of the calibration, which is 8×10^{-4} for the best case I-A. The extrapolation approach is a prediction of the MU outside the traceably calibrated measurement range. The method relies on traceable calibration but it does not replace it. It should only be used when calibration of the full measurement range is not possible. With this extrapolation approach (Weidinger et al., 2023), the MU of the maximum calibration torque in the sub-range is multiplied by a prediction or extrapolation factor that is intended to take the uncertainty of the extrapolation itself into account. The factor is the sum of the scaling factor fs and the classification criteria, as stipulated in DIN 51309, of the class determined in the partial range calibration:

$$f_{\mathrm{s}} = \frac{M_{\mathrm{ex}}}{M_{\mathrm{C}}} \tag{3}$$

$$f_{\mathrm{w}} = f_{\mathrm{s}} + \frac{b}{Y} + \frac{b'}{Y} + \frac{f_0}{Y} + \frac{h}{Y} + \frac{f_{\mathrm{a}}}{Y} + M_{\mathrm{A}} + W_{\mathrm{wCM}} \tag{4}$$

where M_{ex} is the extrapolated torque load step, MC the calibration sub-range, Y the calibration result, MA the lower limit of the measurement range depending on the resolution of the TTS, and W_{wCM} the relative expanded MU of the calibration torque.

Table 1 lists the scaling factor and the weighting factors f_{w} for the 5 MN·m TTS and the extrapolated relative expanded MU using the different prediction factors.

Table 1. Scaling and weighting factor for the 5 MN·m TTS calibrated in the sub-range up to 1.1 MN·m and extrapolated relative expanded MU for the range between 1.5 MN·m and 5 MN·m

Weighted Extrapolation Approach			
Steps	f_{s}	f_{w}	Extrapolated relative expanded MU / %
0	-	-	-
1500	0.11	3.2	0.27
2000	0.15	3.7	0.3
2500	0.19	4.1	0.34
3000	0.23	4.6	0.38
3500	0.26	5	0.42
4000	0.3	5.5	0.45
4500	0.34	5.9	0.49
5000	0.38	6.4	0.53

4.2 Measurement of rotating speed with the mechanical power transfer standard

The first challenge in establishing a transfer standard for measuring rotational speed in nacelle test benches (NTBs) stems from the difficulty of installing the encoder stator in very close proximity to the rotating shaft. This problem is attributed to the towering height of the rotor hub and the absence of rigid structures. To address this, a stator-free method for measuring rotational speed has been developed using a specially chosen inclinometer. This inclinometer, which functions as a micro-electromechanical system (MEMS), contains two perpendicular accelerometers that determine inclination relative to gravity. Placed at the centre of the drivetrain, the inclinometer measures the angular position (ϕ) of the rotating shaft with respect to gravity. The average rotational speed (n) is then calculated based on the change in angle ($\Delta\phi = \phi_2 - \phi_1$) and the elapsed time ($\Delta t$), following the formula:

$$n = \frac{\Delta\phi}{\Delta t} \cdot \frac{60}{360°} \tag{5}$$

The inclinometer's static calibration was performed at the length and angle laboratory at PTB and yielded an expanded MU (with coverage factor $k = 2$) of 0.014° under static conditions using a 0.22 Hz Bessel lowpass filter. Utilising its stator-free characteristic, the inclinometer was mounted on the inner side of the TTS cover plate at the centre part, as depicted in Figure 2.

The overall MU (u_n) of rotational speed is influenced by uncertainties in angle (u_ϕ) and time (u_t), and is determined by the equation:

$$u_\mathrm{n}^2 = \left(\frac{\partial n}{\partial \phi_1} \cdot u_\phi\right)^2 + \left(\frac{\partial n}{\partial \phi_2} \cdot u_\phi\right)^2 + \left(\frac{\partial n}{\partial \Delta t} \cdot u_\mathrm{t}\right)^2 \tag{6}$$

The standard uncertainties of the angle measurement u_ϕ and the time measurement u_t contribute to the total standard uncertainty u_n of the rotational speed measurement:

$$u_\mathrm{n} = \frac{60}{360°} \cdot \sqrt{2\left(\frac{u_\phi}{\Delta t}\right)^2 + \left(\frac{\phi_2 - \phi_1}{\Delta t^2} \cdot u_\mathrm{t}\right)^2} \tag{7}$$

It is obvious that u_n decreases as the time interval Δt increases, thereby reducing uncertainty. To ensure synchronised measurements, rotational speed was measured over the same interval (six revolutions) as the torque measurements.

Incorporating additional uncertainties arising from mounting misalignments, eccentricity, dynamic effects, and data evaluation processes, the total relative expanded uncertainty for rotational speed measurement on the NTB was calculated as 0.02%. Using the aforementioned inclinometer, which was developed as a transfer standard for rotational speed and integrated with the 5 MN·m TTS on the NTB, establishes a traceability chain for rotational speed measurement (Weidinger, 2023).

5 Measurement of electrical output power

Efficiency is the ratio of useful electrical output power converted from the available mechanical input power. Since the output is intended to be fed to the electricity grid, only the electrical power at grid frequency is useful. Power quality phenomena such as other spectral components are relevant since they influence, for instance, the stability of the grid. These are also studied, but

130   since they are not considered "useful output" for determining efficiency, the uncertainty requirements are much less stringent. The setup of the DyNaLab nacelle test bench is shown in simplified form in Figure 3.

In nacelle test benches, electrical power is usually measured using an electrical power measurement system (EPMS) integrated into the test bench's DAQ system. This system is optimised for convenience and versatility, not for minimum uncertainty. Since it is integrated into the nacelle test bench, sending this system to calibration laboratories is difficult and time-consuming.

135   For this reason, METAS (the Swiss national metrology institute) and PTB calibrated a reference power measuring system (RPMS) for use in the test bench. This system is used to determine the efficiency and to calibrate the EPMS measurement chain of the test bench on site.

The RPMS is based on commercial off-the-shelf components such as the LMG671 power analyser and the DL 2000ID current sensors (Figure 3). As the planned reference voltage divider HST12-3 could not be used due to the risk of over-

140   voltage and to test hall safety regulations, the more robust HILO voltage dividers were employed instead, and an extensive recalibration of the HILO sensors had to be carried out at PTB. The over-voltage risk stemmed from the fact that the DUT had to be connected to the medium-voltage grid of the local grid operator instead of to the grid simulator of the test bench. This had the disadvantage that in the event of a fault in the medium-voltage grid, high over-voltages could occur due to ground faults or lightning strikes.

145   The power analyser was used for measurements at the primary side of the transformer. As the primary power standard (Mester, 2021) that is used to calibrate the power analysers, the system is modular. Depending on the currents and voltages to be measured, transducers can be used to reduce the currents and voltages to levels that can be measured with the power analyser. These reference transducers are calibrated with an uncertainty of 300 μV/V and 30 μA/A at power frequency.

Figure 3. Measurement setup of the RPMS and EPMS in the junction box

150 Figure 3 shows that the current measurement chain of the EPMS, consisting of current transformer DS 2000 ICLA, burden resistor HBR1.0, and the HBM data logger GEN4tB with the current measurement card GN8103B, which could be calibrated on site. The MU for the measurement chain is 0.01% and is valid for various load cases. A statement about the long-term stability cannot be made here.

Due to the same over-voltage risk mentioned above, calibration of the HILO sensors on site was also not possible, as the over-voltages would damage the reference sensor of the RPMS. To calibrate the HILO voltage sensors, the entire measurement 155 chain, consisting of voltage divider, connection cable, transmitter, fibre optic cable, and receiver, was shipped to and calibrated in the PTB laboratory (Figure 4) following the test campaign. The calibration was performed as a comparison measurement against a PTB standard. Due to a high position dependence of the voltage divider to other voltage dividers, the calibration resulted in an expanded MU ($k = 2$) of 0.8% at power frequency, with the standard uncertainty being 0.4%.
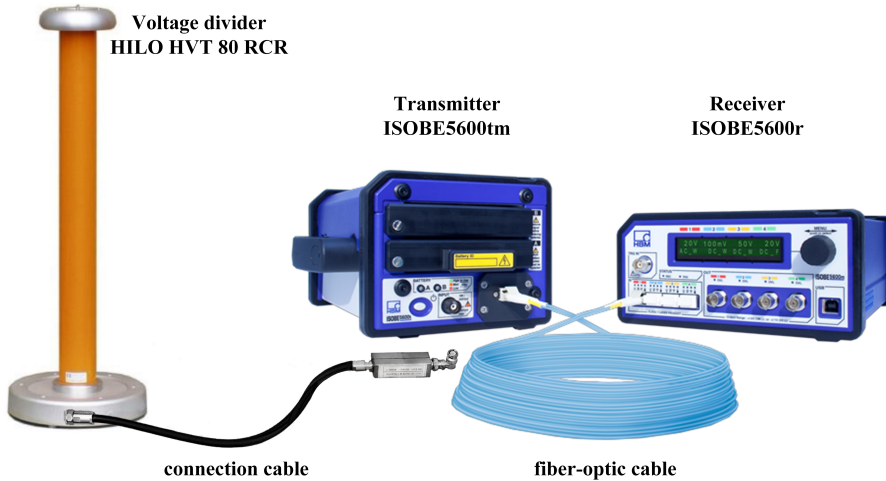
Figure 4. Measuring chain of the EPMS voltage path. Source: https://www.hbm.com/en/2343/isobe5600-isolation-system-standalone-transient-recorder, last access: 26th July 2024, modified by the authors with permission of Hottinger Brüel & Kjaer GmbH

As shown in Table 2, the uncertainty in the voltage measurement plays a dominant role in the overall uncertainty of the 160 electrical power. Thanks to the state-of-the-art sensors and measurement system, the current can be measured with an extremely small uncertainty. Additionally, since the power factor λ of the turbine is kept at 1 during the test, the uncertainty in λ due to the phase errors of voltage and current sensors is negligible. The uncertainties of the three voltage measurements for the three phases are regarded as independent after the calibration and correction. As a result, the total power of the three phases has a smaller relative uncertainty compared to the power of each individual phase.

Table 2. MU of the electrical power measurement

U_1, U_2, U_3	I_1, I_2, I_3	$\lambda_1, \lambda_2, \lambda_3$	P_1, P_2, P_3	P_{elec}
0.40%	0.01%	-	0.40%	0.23%

For the determination of efficiency, the electrical power and mechanical power measurements need to be synchronised. While the mechanical power measurement system is synchronised to UTC using IRIG-B, the chosen RPMS model cannot be synchronised to an external time reference other than by manually setting the time like on a wristwatch. Mechanical imperfections of the nacelle cause a pattern of mechanical power with a period of one revolution. Since the electrical power shows the same pattern, the electrical power measurement is synchronised in a post-processing stage using the cross correlation of the two power measurements.

6 Test results and analysis

During the test campaign, numerous tests serving various purposes were carried out. Because the measurement range of the TTS (5 MN·m) is smaller than the rated torque of the turbine under test, all of the tests were carried with the turbine operating below the rated power. The results of two tests are presented in this paper to demonstrate the method of efficiency determination. In both tests, the torque was held stable around the 5 MN·m level to utilise the maximum capacity of the transducer. In the first test, the rotational speed followed an operational curve in a stepped manner upwards, while in the second test the rotational speed was kept constant to check the long-term behaviour of the turbine. For each test, the mechanical input power and the electrical output power were calculated to determine the efficiency. The uncertainty analysis was carried out for the first test with uncertainty budgets of the raw measurements determined according to the propagation principle.

6.1 Results from warm-up test

In the first test, the turbine was operated at a fixed working point for relatively long periods of time, as shown in Figure 5. This is named the warm-up test and is designed to study the change of temperature and hence the drivetrain efficiency over the course of long-term operation.
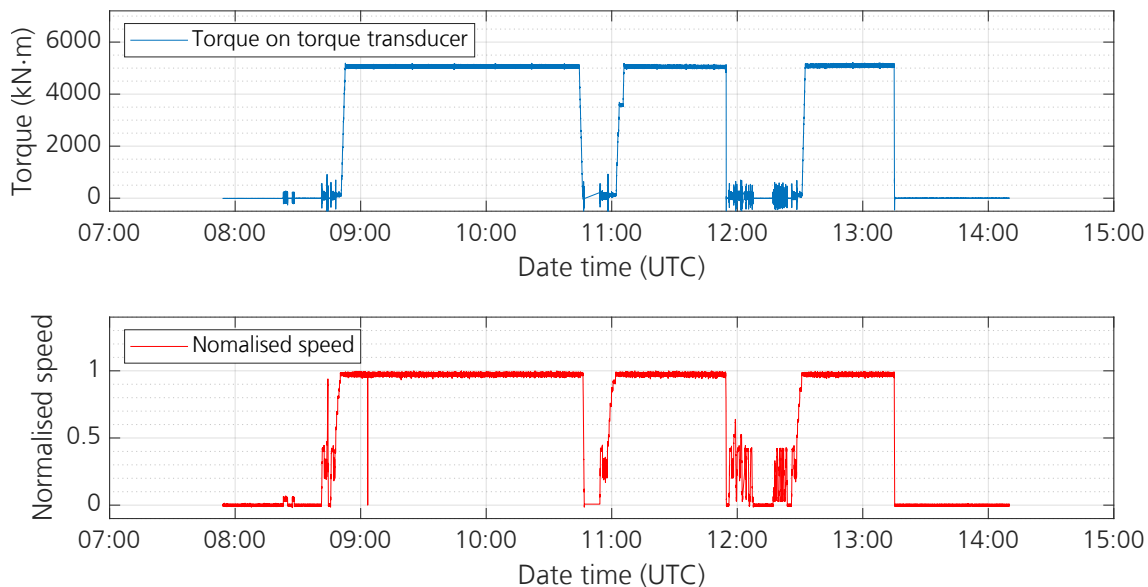
Figure 5. Actual test progress of the warm-up test

Figure 6 shows an overview of efficiency change with progressing operation. For better comparison, the mechanical and
185   electrical power values are shown in the same figure. The general trend of efficiency drop with progressing operation time can
be clearly seen. While the electrical power output is kept constant by means of the control strategy, the mechanical power input
increases slowly. Each point in the upper graph represents the mean value of a 10-revolution power measurement; each point
in the lower graph that of the corresponding efficiency result. The 10-revolution mean values allow better visualisation of the
change trend.
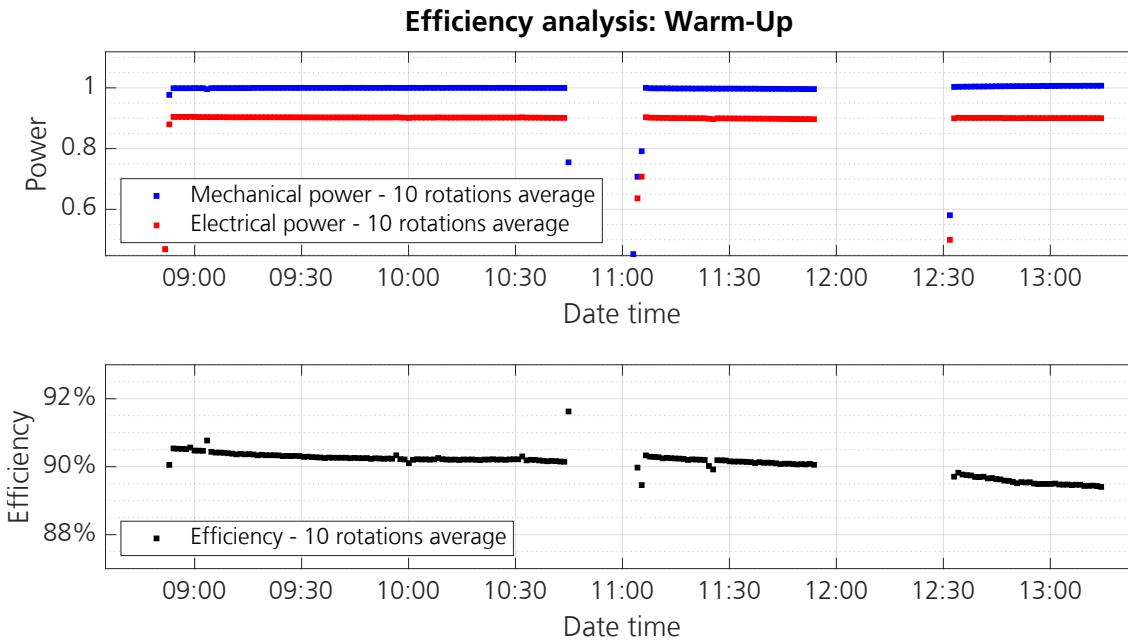
Figure 6. Efficiency determination for the warm-up test

For the reasons listed below, it is difficult, but also not necessary, to measure the instantaneous efficiency. It makes more sense to measure the "mean" efficiency of the drivetrain for one or more revolutions.

- The drivetrain has notable inertia and can store and emit energy as the rotational speed changes.

- The torsional vibration of the drivetrain as well as the speed control strategy cause ripples in the rotational speed.

- The performance of the turbine generator, including its efficiency, is dependent on the air gap distribution between the rotor and stator along the circumference, which varies with the angular position of the rotor.

- The electrical power measurement is only done once per second. The power analyser can calculate the mean power within each second very accurately, but the power between any two outputs needs to be interpolated.

The deviation of the determined efficiency based on a 1-revolution averaged measurement can be calculated provided sufficient data is available. As an example, Figure 7 shows the efficiency determinations based on 100 revolutions. The upper part of the figure shows results of a 1-revolution average η_1, with the standard deviation of the 100 points being 0.13%. In the lower part of the figure, the efficiency was determined for every 10 revolutions of measurement, η_{10}, resulting in 10 points in the plot. The standard deviation of these 10 points is 0.019%.
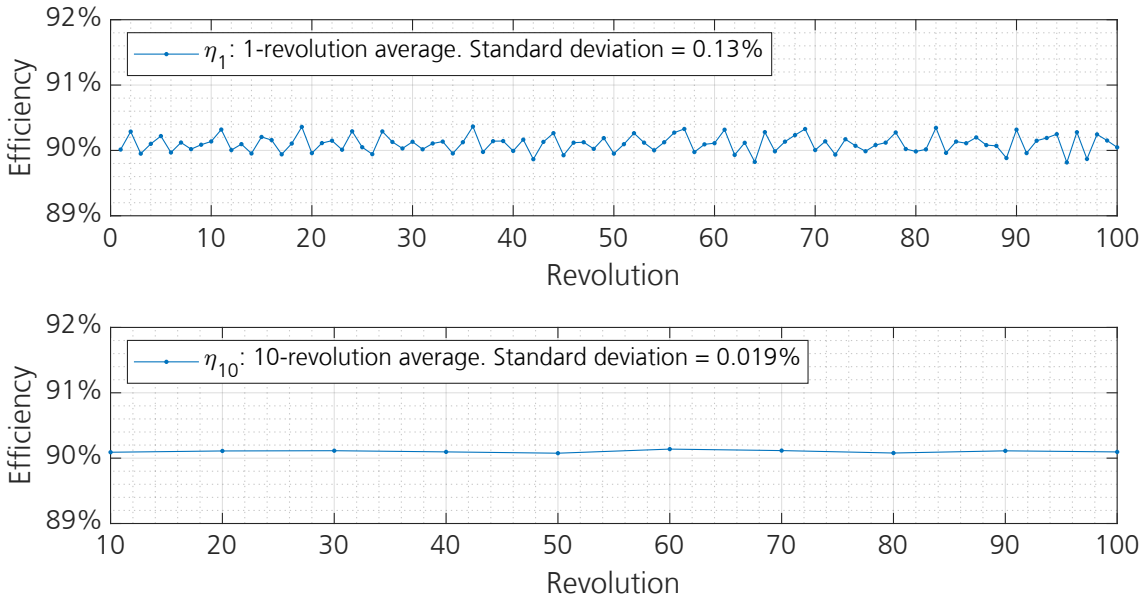
Figure 7. Standard deviation of 1-revolution and 10-revolution averaged efficiency. The very small drift of efficiency at different revolutions is compensated by a detrend operation in Matlab

The standard deviations of η_1 and η_{10} are denoted as σ_{η_1} and $\sigma_{\eta_{10}}$. A comparison between the two is given in Table 3. According to the GUM guideline (JCGM, 2008), $\sigma_{\eta_{10}}$ would be equal to σ_{η_1} divided by $\sqrt{10}$ if the uncertainties of the determined η_1 values are independent from each other. It should be noted, however, that $\sigma_{\eta_{10}}$ is much smaller than $\sigma_{\eta_1}/\sqrt{10}$, as shown in Table 3.

Table 3. Comparison of standard deviations of η_1 and η_{10}

σ_{η_1}	$\sigma_{\eta_1}/\sqrt{10}$	$\sigma_{\eta_{10}}$
0.13%	0.04%	0.019%

This indicates that in this case the determined values of efficiency with single revolution measurement η_1 are not independent in terms of measurement uncertainty. Nevertheless, since $\sigma_{\eta_1}/\sqrt{10}$ gives a larger uncertainty than $\sigma_{\eta_{10}}$, and σ_{η_1} needs a much smaller period of measurement to calculate than $\sigma_{\eta_{10}}$, it remains meaningful to use $\sigma_{\eta_1}/\sqrt{10}$ as a conservative estimation (Equation 8) of $\sigma_{\eta_{10}}$ if the measurement period or the number of revolutions is limited.

$$\sigma^*_{\eta_{10}} = \sigma_{\eta_1}/\sqrt{10} \tag{8}$$

The detailed uncertainty budget for the determined efficiency with the averaged measurement of 10 revolutions is shown in Table 4. The left side of the table presents the uncertainty contributions from the measured electrical and mechanical variables. These are used to determine the efficiency uncertainty associated solely with the measurement chains and denoted as $u_{\eta,\text{meas}}$.

215 On the right side of the table, the uncertainty associated with the instability in the efficiency is indicated, with the standard deviation adopted as the standard uncertainty $u_{\eta_{10},\text{ins}}$. In this case, the 10-revolution average is used. If the efficiency is determined with the average of a different number of revolutions, the corresponding standard deviation should be used.

Table 4. Overall uncertainty budget of the determined drivetrain efficiency

Current	Voltage	Torque	Speed	
$u_{\text{I}} = 0.01\%$	$u_{\text{V}} = 0.4\%$	$u_{\text{T}} = 0.27\%$	$u_{\text{n}} = 0.01\%$	Instability in efficiency
Electrical power		Mechanical power		
$u_{\text{P}_{\text{elec}}} = 0.23\%$		$u_{\text{P}_{\text{mech}}} = 0.27\%$		
Uncertainty caused by measurement chains				$u_{\eta_{10},\text{ins}} = \sigma^{*}_{\eta_{10}} = 0.041\%$
$u_{\eta,\text{meas}} = 0.35\%$				
Overall				
$u_{\eta_{10}} = 0.35\%$, expanded uncertainty $U_{\eta_{10}} = 0.70\% \ (k = 2)$				

Combining the contributions of measurement chains and the instability yields the overall uncertainty in efficiency shown at the bottom of the table. Obviously, the contribution of instability in this case plays only a negligible role in the uncertainty of 220 the determined efficiency based on a 10-revolution averaged measurement.

6.2 Operational curve test

In the second test, the rotational speed followed a 27-step profile up to the rated speed, while the torque was kept at the nominal level of the TTS, namely 5 MN·m. Figure 8 shows the actual test progress. Since only a limited number of revolutions were available on each step, the efficiency shown in Figure 9 was calculated with the average of just one revolution, denoted as 225 η_1. For each step, calculation was done based on the data from six revolutions, so six efficiency points, each representing the average of a single revolution, are shown. Within each step, the deviation of the six η_1 points is clearly shown. The standard deviation σ_{η_1} for each test step can be calculated using the corresponding six points.
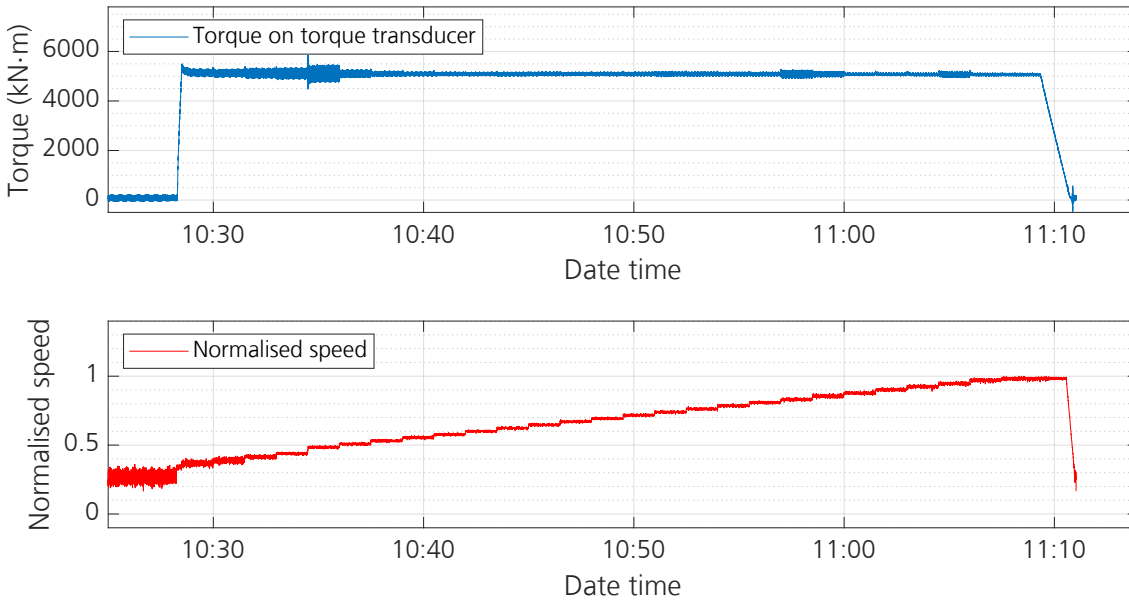
Figure 8. Actual test progress of the operational curve test
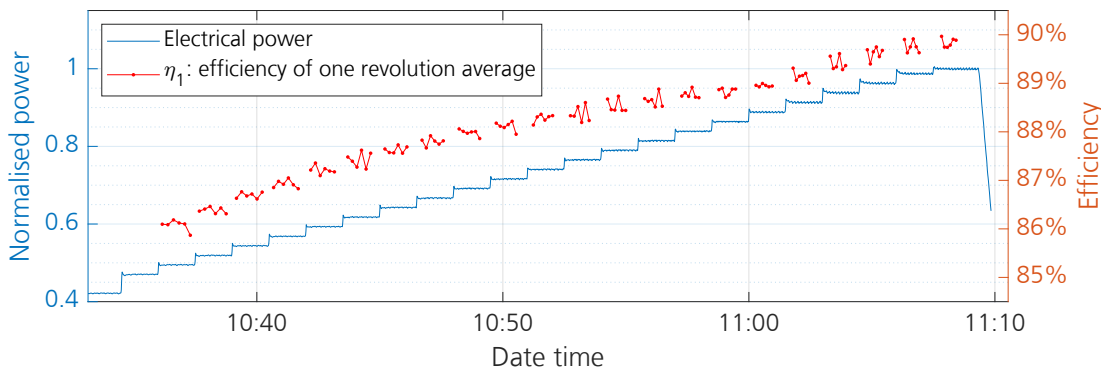
Figure 9. Efficiency of one revolution average for the operational test

To obtain the efficiency of each test step, the measurements of all six revolutions were used to determine the six-revolution averaged efficiency η_6. As pointed out by Song et al. (2023), the measurements of at least six full revolutions should be averaged to achieve a good level of accuracy. The results of σ_{η_6} for some of the test steps are listed in Table 5. Since there were not enough revolutions to determine the standard deviation σ_{η_6}, the value of σ_{η_1} is used instead for the calculation of the uncertainty. It is worth pointing out here that the standard deviation of a single revolution's average efficiency is adopted directly instead of in a form similar to Equation 8. This is because six points represent a very limited basis to obtain a reliable calculation of σ_{η_1}. Using σ_{η_1} directly as σ_{η_6} serves to yield conservative results in the uncertainty analysis. The overall uncertainty of the determined efficiency is also given in Table 5. Since the torque remains at 5 MN·m throughout all the test steps, the uncertainty

due to the measurement chains is identical to the value in Table 4 for all the steps: $u_{\eta,\mathrm{meas}} = 0.35\%$. This is therefore not listed again in Table 5. The results show that $u_{\eta,\mathrm{meas}}$ plays a dominant role in the uncertainty of the efficiency.

Table 5. Determined efficiency and its uncertainty of some of the test steps

Step	7	11	15	19	23	27
Speed (normalised)	0.54	0.64	0.73	0.82	0.92	1.00
η_6	86.38%	87.43%	88.12%	88.65%	89.15%	89.84%
$u_{\mathrm{ins}} = \sigma_{\eta_1}$	0.06%	0.16%	0.09%	0.13%	0.11%	0.09%
$U_{\eta_6}(k=2)$	0.72%	0.76%	0.72%	0.74%	0.74%	0.72%

7 Discussion

The efficiency determination for both of the tests discussed above achieved an accuracy of approximately 0.7% uncertainty, thereby breaking the 1% mark. The largest uncertainty contribution still comes from the torque measurement, despite the use of the best possible torque transducer and calibration machine. To further reduce the uncertainty, the transducer needs to be calibrated to a higher level of torque. PTB is commissioning a new torque calibration machine with a capacity of 5 MN·m, and this could help achieve better uncertainty.

The second largest contribution comes from the voltage measurement. Although in this case it stems from safety regulation requirements and could in the particular circumstances be solved by a dedicated reconfiguration of the test bench, it still shows the importance of planning effort and investment in electrical power measurement. In practice, it should not be taken for granted that electrical power can be measured automatically with sufficient accuracy. Because testing time on a nacelle test bench is a limited resource (drivetrain efficiency would very likely be tested together with many other test items), it is not always possible to reconfigure the test layout just for one test. Therefore, it is important to plan the test in advance and take all relevant factors into consideration in order to achieve the best possible electrical measurement accuracy.

Rotational speed and electrical current measurements achieved very high levels of accuracy. For these two cases, suitable sensors with careful calibration were instrumented at the right positions on the drivetrain and integrated into well calibrated measurement chains. All these factors combined to produce satisfying results.

Owing to a number of discussed reasons, ripples on the measurement and deviations in the determined efficiency are inevitable. To achieve stable efficiency under certain conditions, it is recommended to average at least six full revolutions of measurement. Based on the results of this study, the uncertainty caused by the deviation in efficiency will only represent a minor contributor to the overall uncertainty of efficiency if this recommendation is followed.

One limitation of the test layout presented in this paper is that the non-torque loads, such as bending moments and shear forces, could not be applied to the DUT because the 5 MN·m TTS from PTB is not designed to withstand high levels of non-torque loads. To overcome this limitation, a series of calibration profiles was carried out during the test campaign so that a transducer developed in-house at PTB could be calibrated on the DyNaLab. This transducer was placed directly in front of

the reference transducer from PTB. The torque calibration of this transducer has been reported by Zhang et al. (2023). This transducer is designed to withstand and measure loads in all six degrees of freedom and will be used for torque measurement in future test campaigns.

8 Conclusions

This paper reported an approach to determine the drivetrain efficiency of a modern multi-MW wind turbine. Addressing the challenge of measurement accuracy, state-of-the-art sensors, measurement systems, and calibration facilities were employed within the framework the WindEFCY project. The results show that an overall uncertainty level of 0.7% is achievable for efficiency determination with torque measurement up to 5 MN·m. As expected, torque measurement contributed the largest share of the uncertainty. Surprisingly, electrical power measurement also made a large uncertainty contribution. This highlights the fact that although electrical measurements are generally considered to be much more accurate, equal care must be exercised when measuring both electrical and mechanical power. Speed measurement based on the inclinometer yielded very good results. To achieve a stable efficiency, the measurement of at least six full revolutions was averaged, resulting in nearly negligible contributions to the overall uncertainty.

Author contributions. HZ concepted the paper, carried out the data analysis and wrote the major part of the paper. PW and ZS were responsible for torque and speed measurement, as well as the corresponding text in this paper. CM and AD were responsible for electrical power measurement, as well as the corresponding text in this paper. AD also carried out the comprehensive calibration of the HILO voltage dividers. MH and KE coordinated the project and test execution, BT took part in the sensor instrumentation.

Competing interests. No competing interests exist.

Acknowledgements. The project 19ENG08 – WindEFCY has received funding from the EMPIR programme co-financed by the Participating States from the European Union's Horizon 2020 research and innovation programme. The input of all the project partners is gratefully acknowledged.

References

Foyer, G., Kock, S., and Weidinger, P.: Influences on torque measurement in nacelle test benches and their effect on the measurement uncertainty and consequences of a torque calibration, ACTA IMEKO, 8, 59, https://doi.org/10.21014/acta_imeko.v8i3.658, 2019.

JCGM: Evaluation of measurement data – Guide to the Expression of Uncertainty in Measurement (GUM), Standard, Joint Committee for Guides in Metrology JCGM, 2008.

Mester, C.: Sampling Primary Power Standard from DC up to 9 kHz Using Commercial Off-The-Shelf Components, Energies, 14, https://doi.org/10.3390/en14082203, 2021.

Pagitsch, M., Jacobs, G., Schelenz, R., Bosse, D., Liewen, C., Reisch, S., and Deicke, M.: Feasibility of large-scale calorimetric efficiency measurement for wind turbine generator drivetrains, Journal of Physics: Conference Series, 753, 072 011, https://doi.org/10.1088/1742-6596/753/7/072011, 2016.

Song, Z., Weidinger, P., Zhang, H., Heller, M., Oliveira, R., and Kumme, R.: Metrological characterisation of rotational speed measurement using an inclinometer in a nacelle test bench, in: 21. ITG/GMA Fachtagung Sensoren und Messsysteme, 2022.

Song, Z., Weidinger, P., Zweiffel, M., Dubowik, A., Mester, C., Yogal, N., and Oliveira, R.: Traceable efficiency determination of a 2.75 MW nacelle on a test bench, Forschung im Ingenieurwesen, 87, https://doi.org/10.1007/s10010-023-00650-1, 2023.

Weidinger, P., Schlegel, C., Foyer, G., and Kumme, R.: Characterisation of a 5 MN·m torque transducer by combining traditional calibration and finite element method simulations, in: AMA Conferences, doi: 10.5162/sensor2017/D6.2, 2017.

Weidinger, P., Dubowik, A., Lehrmann, C., Yogal, N., Kumme, R., Zweiffel, M., Eich, N., Mester, C., and Zhang, H.: Need for a traceable efficiency determination method of nacelles performed on test benches, Measurement: Sensors, 18, 100 159, https://doi.org/https://doi.org/10.1016/j.measen.2021.100159, 2021.

Weidinger, P., Song, Z., Oliveira, R. S. d., Vavrečka, L., Fidelus, J., Kananen, T., Heller, M., and Zhang, H.: Deliverable D3 within 19ENG08, https://doi.org/10.5281/zenodo.8112428, 2023.

Weidinger, P. e. a.: Deliverable D4 within 19ENG08 Good Practice Guide on the calibration procedure for traceable mechanical power measurement based on synchronised torque and rotational speed measurement, Tech. rep., zenodo, 2023.

Zhang, H. and Neshati, M.: An effective method of determining the drive-train effciency of wind turbines with high accuracy, Journal of Physics: Conference Series, 1037, 052 013, https://doi.org/10.1088/1742-6596/1037/5/052013, 2018.

Zhang, H., Pieper, S., and Heller, M.: Direct measurement of input loads for the wind turbine drivetrain under test on a nacelle test bench, Forschung im Ingenieurwesen, 87, https://doi.org/10.1007/s10010-023-00628-z, 2023.